Particle Accelerators, 1992, Vol. 36, pp. 251–270
Reprints available directly from the publisher
Photocopying permitted by license only

TRANSFORMATION AND INTERACTION OF ELECTROMAGNETIC PULSES WITH AN ELECTRON BEAM IN RADIAL TRANSMISSION LINES

V. V. ZAKUTIN and A. M. SHENDEROVICH

Kharkov Institute of Physics and Technology,
Ukrainian Academy of Sciences, 310108 Kharkov, Ukraine.

(*Received 30 March 1990; in final form 20 August 1991*)

This paper is devoted to a detailed theoretical and experimental investigation of the processes occurring during propagation of brief electromagnetic pulses in radial transmission lines. The main mechanism of pulse amplitude and time transformation have been studied. The amplitude transformation effect is shown to depend on the wave transit time, electric-field rise time at the line input, and the magnetic relaxation time of ferrite placed inside the radial line. A gain of 360 keV in the electron energy has been obtained in a system involving three radial lines at a supply voltage of 38 kV. The time-transformation effect may be used to generate short (sub-nanosecond) electric pulses.

1 INTRODUCTION

In the last few years much attention has been given to accelerating structures relying on radial lines driven by an external pulse generator.[1–6] The interest in these structures comes from the fact that, on propagating from the periphery to the center of the radial line, the electromagnetic pulse grows in amplitude.[1–3] Consequently, the electron beam traversing along the axis of a sequence of radial lines is influenced by an accelerating voltage in the cell considerably exceeding the supply voltage. It is reasonable to employ radial lines loaded with ferrite to reduce substantially the overall dimensions of the accelerating structure, for relatively long pulses. As the electromagnetic pulse propagates inward its duration is reduced; this effect can be used to obtain short accelerating pulses.

This paper presents a detailed theoretical and experimental description of the amplitude and time transformation of electromagnetic pulses in their propagation from the periphery to the center of the radial line, and of their interaction with an electron beam.

In Sections 2 to 4 we consider the amplitude transformation and beam interaction of electromagnetic pulses in a single radial line and in a sequence of such lines. Section 2 gives a theoretical analysis of electromagnetic pulse propagation in a radial line. As a result, a complete space-time distribution pattern is constructed for the electric and magnetic fields in the radial lines as a function of the parameters of the driving pulse, the radial line, and the loading material. In particular, magnetic relaxation in

ferrite is treated. Sections 3 and 4 present the experimental results for the transformation of pulse amplitudes in the radial lines with and without ferrite. Electron beam acceleration is studied in a single radial line and in an array of them. The influence of the beam on transformation effects is also investigated.

In Section 5 we study the time transformation of electromagnetic pulses in a radial line. The inverse problem is solved for finding the necessary amplitude and shape of the supply voltage pulse in order to obtain the assigned pulse amplitude and shape on the axis of the line. The possibility of obtaining pulses of sub-nanosecond duration with a relatively long supply voltage pulse is demonstrated by both calculations and measurements.

2 ANALYSIS OF PULSE AMPLITUDE TRANSFORMATION IN A RADIAL TRANSMISSION LINE

Let us consider the transformation processes of an electromagnetic pulse propagating from the periphery to the center of a radial transmission line (Figure 1). The radial line has two metal disks (1) of a radius R and a ferrite element (2) of thickness d between the disks. The line is uniformly driven from outside by a pulse voltage source $U(t)$ with impedance ρ.

The analysis (in Gaussian system of units) is based on the joint solution of Maxwell's equations and Bloch's equation for ferrite magnetization:[7]

$$\frac{d\mathbf{M}}{dt} = \frac{1}{\tau_\rho}(\chi\mathbf{H} - \mathbf{M}), \tag{1}$$

where $\mathbf{H}$ is the magnetic field of the electromagnetic wave; $\mathbf{M}$, χ, and τ_ρ are, respectively, the magnetization, magnetic susceptibility, and relaxation time of the ferrite. For the Fourier component of the electric ($E_{\omega z}$) and magnetic ($H_{\omega\varphi}$) fields of

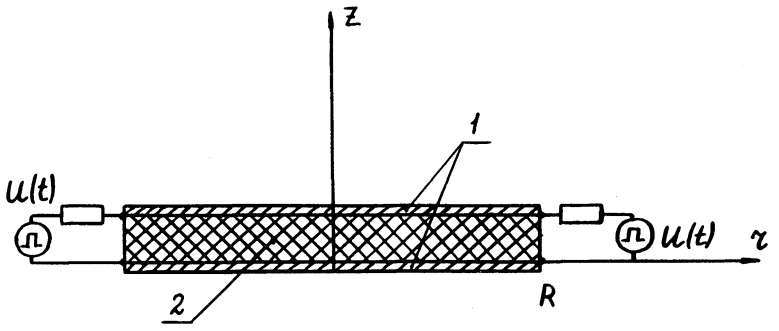

FIGURE 1 Radial transmission line.

the TM_{010} wave at radial distance r, it is easy to derive the following expressions:

$$E_{\omega z}(r) = \frac{A}{i} J_0\left(\frac{\omega}{c}\sqrt{\varepsilon}\sqrt{1+\frac{4\pi\chi}{1+i\omega\tau_\rho}}\,r\right), \tag{2}$$

$$H_{\omega\varphi}(r) = \frac{\sqrt{\varepsilon}}{\sqrt{1+\frac{4\pi\chi}{1+i\omega\tau_\rho}}} A J_1\left(\frac{\omega}{c}\sqrt{\varepsilon}\sqrt{1+\frac{4\pi\chi}{1+i\omega\tau_\rho}}\,r\right), \tag{3}$$

where ω is the frequency, ε is the dielectric constant of the ferrite, c is the speed of light, and J_0 and J_1 are the Bessel functions. Proceeding from Ohm's law, we get the boundary conditions at an external radial distance R:

$$U_\omega = E_\omega d = \rho J_\omega + E_\omega(R)d = \frac{\rho c R}{2} H_{\omega\varphi}(R) + E_\omega(R)d, \tag{4}$$

where d is the disk spacing of the radial line; U_ω, I_ω, and E_ω are the Fourier components of voltage $U(t)$, the current and the electric field at the line input, respectively. Equation (4) is derived by the use of the relationship $I_\omega = (cR/2)H_{\omega\varphi}(R)$, which is a consequence of the boundary condition at the external radius rot $\mathbf{H} = (4\pi/c)j$ (j is the current density). From Eq. (2), and with Eq. (4) in view, we obtain,

$$E_{\omega z} = \frac{E_\omega J_0\left(\frac{\omega}{c}\sqrt{\varepsilon}\sqrt{1+\frac{4\pi\chi}{1+i\omega\tau_\rho}}\,r\right)}{\left\{J_0\left(\frac{\omega}{c}\sqrt{\varepsilon}\sqrt{1+\frac{4\pi\chi}{1+i\omega\tau_\rho}}\,R\right) + i\frac{\rho c R}{2}\cdot\frac{\sqrt{\varepsilon}}{\sqrt{1+\frac{4\pi\chi}{1+i\omega\tau_\rho}}} J_1\left(\frac{\omega}{c}\sqrt{\varepsilon}\sqrt{1+\frac{4\pi\chi}{1+i\omega\tau_\rho}}\,R\right)\right\}} \tag{5}$$

$$H_{\omega\varphi} = i\frac{E_\omega\sqrt{\varepsilon}\,J_1\left(\frac{\omega}{c}\sqrt{\varepsilon}\sqrt{1+\frac{4\pi\chi}{1+\omega\tau_\rho}}\,r\right)}{\left\{\sqrt{1+\frac{4\pi\chi}{1+i\omega\tau_\rho}}\left\{J_0\left(\frac{\omega}{c}\sqrt{\varepsilon}\sqrt{1+\frac{4\pi\chi}{1+i\omega\tau_\rho}}\,R\right) + \frac{i\rho c R}{2}\frac{\sqrt{\varepsilon}}{\sqrt{1+\frac{4\pi\chi}{1+i\omega\tau_\rho}}} J_1\left(\frac{\omega}{c}\sqrt{\varepsilon}\sqrt{1+\frac{4\pi\chi}{i\omega\tau_\rho}}\,R\right)\right\}\right\}}. \tag{6}$$

Let us consider the amplitude and shape transformation of a trapezoidal pulse of amplitude E_0 with a rise time η, fall time ξ, and flat-top duration T. Calculating

the Fourier-transformed image of this pulse, then substituting it into Eqs (5) and (6) and calculating the Fourier integrals, we obtain the following expressions for the electric and magnetic fields at $\rho = 0$ and a small relaxation time ($\omega\tau_\rho \ll 1$, $\omega^2\tau_\rho(R/c)\sqrt{\varepsilon(1+4\pi\chi)} \ll 1$):

$$\left.\begin{aligned} E_z &= E\left(\frac{t}{\theta}\right) \\ H_\varphi &= H\left(\frac{t}{\theta}\right) \end{aligned}\right\} 0 \le \frac{t}{\theta} \le \frac{\eta}{\theta}$$

$$\left.\begin{aligned} E_z &= E\left(\frac{t}{\theta}\right) - E\left(\frac{t-\eta}{\theta}\right) \\ H_\phi &= H\left(\frac{t}{\theta}\right) - H\left(\frac{t-\eta}{\theta}\right) \end{aligned}\right\} \frac{\eta}{\theta} \le \frac{t}{\theta} \le \frac{\eta+T}{\theta}$$

$$\left.\begin{aligned} E_z &= E\left(\frac{t}{\theta}\right) - E\left(\frac{t-\eta}{\theta}\right) + E\left(\frac{t-\eta-T}{\theta}\right) \\ H_\varphi &= H\left(\frac{t}{\theta}\right) - H\left(\frac{t-\eta}{\theta}\right) + H\left(\frac{t-\eta-T}{\theta}\right) \end{aligned}\right\} \frac{\eta+T}{\theta} \le \frac{t}{\theta} \le \frac{\eta+T+\xi}{\theta} \tag{7}$$

$$\left.\begin{aligned} E_z &= E\left(\frac{t}{\theta}\right) - E\left(\frac{t-\eta}{\theta}\right) + E\left(\frac{t-\eta-T}{\theta}\right) - E\left(\frac{t-\eta-T-\xi}{\theta}\right) \\ H_\varphi &= H\left(\frac{t}{\theta}\right) - H\left(\frac{t-\eta}{\theta}\right) + H\left(\frac{t-\eta-T}{\theta}\right) - H\left(\frac{t-\eta-T-\xi}{\theta}\right) \end{aligned}\right\} \frac{\eta+T+\xi}{\theta} \le \frac{t}{\theta},$$

where

$$E\left(\frac{t}{\theta}\right) = E_0 \frac{\theta}{\eta}\left\{\frac{t}{\theta} - \sum_{n=1}^{\infty} \frac{e^{-(\sigma_n^2/2)(\tau_\rho/\theta)(t/\theta)}}{\sigma_n^2 J_1(\sigma_n)} \times \left[2J_0\left(\sigma_n \frac{r}{R}\right) \sin \sigma_n \frac{t}{\theta} + \frac{\tau_\rho}{\theta} \sigma_n^2 \frac{r}{R} J_1\left(\sigma_n \frac{r}{R}\right) \cos \sigma_n \frac{t}{\theta}\right]\right\} \tag{8}$$

and

$$H\left(\frac{t}{\theta}\right) = E_0 \frac{\theta}{\eta}\sqrt{\frac{\varepsilon}{\mu_0}}\left\{\frac{r}{2R} + \sum_{n=1}^{\infty} \frac{e^{-(\sigma_n^2/2)(\tau_\rho/\theta)(t/\theta)}}{\sigma_n^2 J_1(\sigma_n)}\left[-2J_1\left(\sigma_n \frac{r}{R}\right) \cos \sigma_n \frac{t}{\theta} + \frac{\tau_\rho}{\theta} \sigma_n^2 \frac{r}{R} J_0\left(\sigma_n \frac{r}{R}\right) \sin \sigma_n \frac{t}{\theta}\right]\right\}. \tag{9}$$

Here $\theta = (R/c)\sqrt{\varepsilon\mu_0}$ is the total transit time of the wave, $\mu_0 = 1 + 4\pi\chi$ is the magnetic permeability of the ferrite, and σ_n are the roots of the function J_0.

The above expressions can be used to find out the main regularities of transformation effects as functions of excitation conditions and radial-line parameters.

For the particular case of $\eta \to \infty$, Eq. (8) obviously gives $E_z/E_0 = 1$, i.e., at an infinite pulse rise time, the transformation of amplitude does not occur.

In the other limiting case, $\eta \to 0$, Eq. (8) changes to the expression derived in Ref. 2 for the electric field at $\tau_p = 0$:

$$\frac{E_z}{E_0} = 1 - 2\sum_{n=1}^{\infty} \frac{\cos \sigma_n \dfrac{t}{\theta}}{\sigma_n J_1(\sigma_n)}. \tag{10}$$

We first consider the transformation effects at $\tau_p = 0$. Figure 2 shows the calculated space-time distribution of the electric field in the radial transmission line. It is seen that during inward propagation, the pulse amplitude grows substantially while the length of the pulse is reduced. The calculations of Eqns. (8) and (9) have shown that, with a shorter pulse length, shape distortion becomes less significant and the shape of small-duration pulses remains practically the same during pulse propagation within the distance $R/3$. From Eqns. (8) and (9) it follows that the pulse amplitude transformation effect depends only on the relationship between the wave-transit time along the line θ and the pulse risetime η at the line input. The generalized dependence

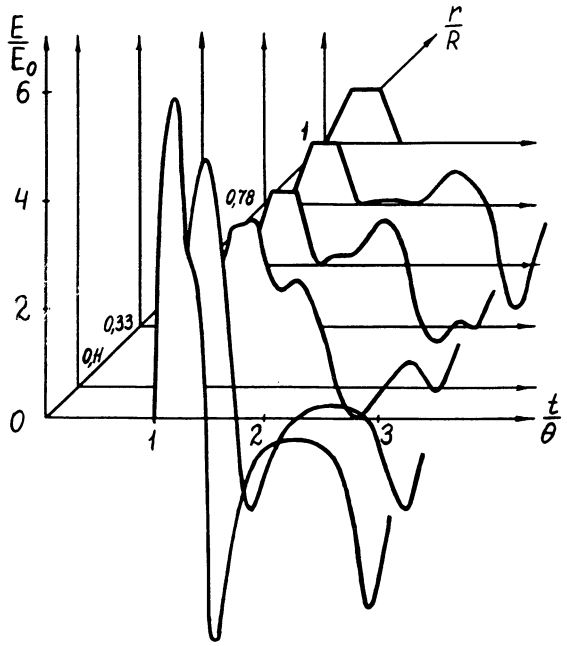

FIGURE 2 Time dependence of the electric field at different radii of the radial line (r/R = 1, 0.78, 0.55, 0.33, 0.11, and 0) at $\theta/\eta = 4.5$, $T/\theta = 0.22$.

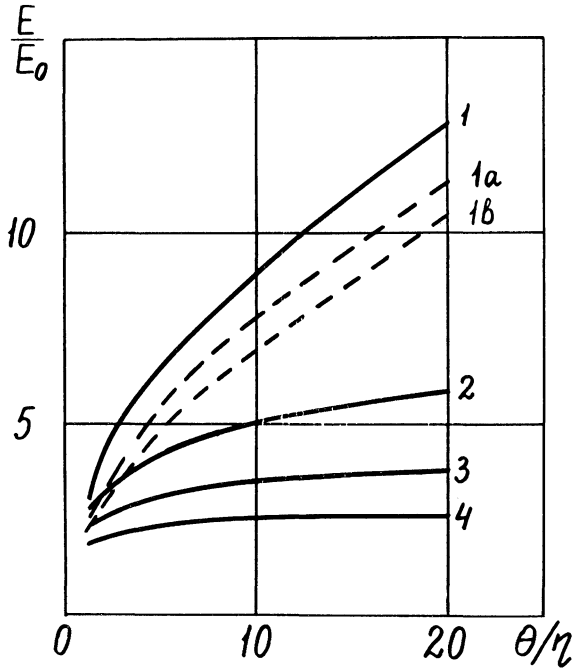

FIGURE 3 Dependence of the electric field in the radial line on the θ/η ratio for $r/R = 0$ (curve 1), 0.11 (curve 2) 0.33 (curve 3), and 0.55 (curve 4). (1a) $r/R = 0$, $\tau_p/\theta = 1 \times 10^{-4}$; (1b) $r/R = 0$, $\tau_p/\theta = 5 \times 10^{-4}$.

of the electric-field amplitude on this relation at different line radii is shown in Figure 3. It may be seen from the figure that the transformation of pulse amplitude may be rather large, e.g., at $\theta/\eta = 5$, the electric-field value on the axis is greater by a factor of 6.3 than that at the line input. It is also seen that, in the center of the line, the transformation effect depends strongly on the θ/η ratio, whereas from $r/R \approx 0.3$ the θ/η dependence of the effect is substantially weaker.

The ferrite loading of the radial transmission line enables one to greatly reduce its transverse dimensions. In this case, in calculations it is necessary to take into account a magnetic relaxation in ferrite which may cause the accelerating—field pulse amplitude and shape to change. The dashed line in Figure 3 shows the amplitude of the electric field on the line axis ($r = 0$) as a function of the magnetic relaxation time τ_ρ. The pulse shape on the radial line axis at a finite magnetic relaxation time is shown in Figure 4. As may be seen from Figures 3 and 4, magnetic relaxation spreads out the pulse and reduces its amplitude. The present analysis shows the magnetic relaxation time, at which the pulse amplitude and shape remain practically the same, to be $\tau_\rho \sim 10^{-3}\,\theta$. As demonstrated in Section 4, this is quite feasible at sufficiently great fields.

The calculated magnetic field distribution of the electromagnetic electronetic pulse along the line varies, depending on the θ/η ratio (Figure 5). At a low θ/η value, the magnetic field amplitude falls off smoothly to zero from the periphery to the center of the line (curves 1 and 2). At a large θ/η ratio value, as the pulse propagates to the

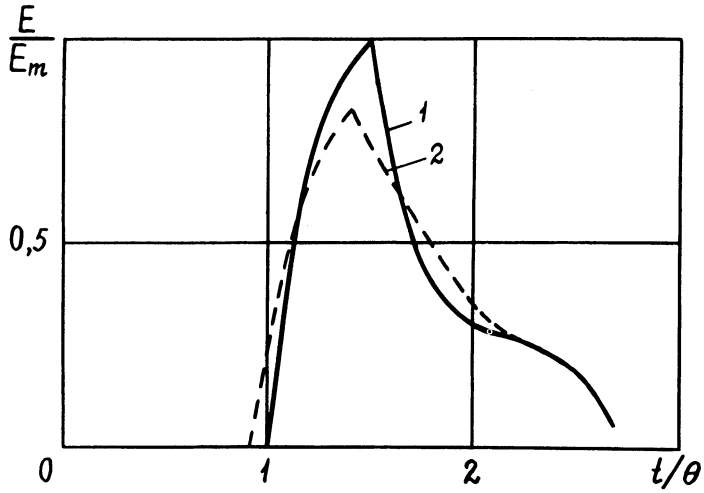

FIGURE 4 Pulses on the line axis ($r/R = 0$). (1) $\theta/\eta = 2$, $\tau_p/\theta = 0$; (2) $\theta/\eta = 2$, $\tau_p/\theta = 0.06$.

line axis, the magnetic field first increases and then falls off to zero; the greatest magnetic field value is observed at short rise times, its maximum position shifting closer to the line axis. The data shown in Figure 5 allows one, in particular, to determine the restrictions due to ferrite saturation by the magnetic field of the electromagnetic wave during transformation of powerful pulses. At a given θ/η (using the curves in Figure 5) we first determine the maximum $H_m/10H_0$ ratio and then, by calculating $H_0 = 0.15E_0\sqrt{\varepsilon/\mu_0}$, we find the greatest magnetic field H_m of the pulse

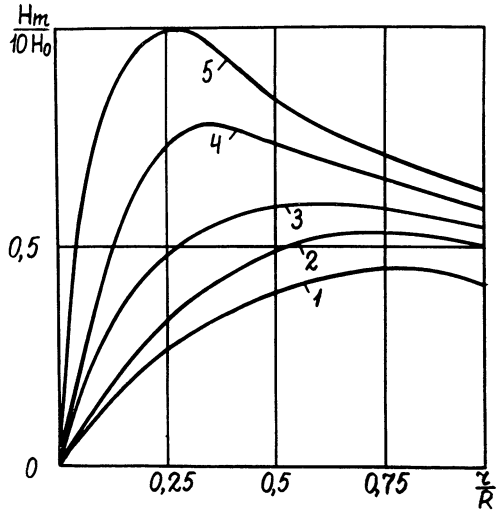

FIGURE 5 Magnetic field amplitude distribution at a radial distance for $\theta/\eta = 0.9$ (1), 1.15 (2), 1.5 (3), 2.25 (4), 4.5 (5). $H_0 = 0.15E_0\sqrt{\varepsilon/\mu_0}$.

in the ferrite. The H_m value should be lower than the magnetic field of ferrite saturation.

In the above analysis we have found the mechanism of pulse amplitude transformation in the radial transmission line, which involves the compression of the electromagnetic field during pulse propagation inwards and energy transfer from the magnetic field of the wave to the electric field near the line axis. The amplitude transformation is shown to attain significant values.

3 EXPERIMENTAL STUDIES OF PULSE AMPLITUDE TRANSFORMATION IN THE RADIAL LINE

Pulse amplitude transformation effects were experimentally investigated in radial lines with and without ferrite, thereby providing favorable conditions to elucidate the role of magnetic relaxation. The radial line containing no ferrite had an external radius $R = 90$ cm ($\theta = 3$ ns), the distance between the disks d varied from 2 to 13 cm, and the radius of the hole in the center of the line was $a = 1$ cm. The type 60 NN ($B_m = 4200\ G$, $\mu = 60$, $f_m = 55$ MHz) ferrite-loaded radial line measured only $R = 9$ cm ($\theta = 4.5$ ns), $d = 2$ cm, $a = 3$ cm. The hole dimensions in the center of the line were small as compared with the minimal wavelength in the pulse spectrum; therefore the above calculations for the "solid" line are applicable to describing the present experiments. This is confirmed by the measured data given below. The lines were driven by a pulse generator with a pulse of amplitude $U = 1$ kV, and the pulse rise time η ranged from 1 to 10 ns. The pulse from the generator was applied to the input of the radial line at regular radial spacings at 24 points through 50-ohm cables, each 6 m long. The voltage pulse in the center of the line was supplied, via a divider, to an oscillograph. The time resolution of the measuring system was better than or equal to 0.5 ns.

Figure 6 shows the amplitude transformation effect in the radial line without ferrite as a function of η (experimental data points on curve 1). The results of the measurements agree with the calculation (curve 1) and thus confirm the conclusion of the theoretical analysis that the transformation effect increases with the θ/η ratio.

The same figure shows the measured transformation values for the ferrite-loaded line. These results differ from the calculated values at $\tau_\rho = 0$ (curve 2) and are in agreement with the calculations for $\tau_\rho/\theta = 0.067$, i.e., $\tau_\rho = 0.3$ ns (curve 3). Besides, the measurements have shown that the electric-field pulse shape also agrees with the calculated one for the given relaxation time. It may be seen from Figure 6 that in accordance with the calculations, the pulse amplitude decreases under the influence of the magnetic relaxation in ferrite is especially significant at small η, e.g., at $\theta/\eta = 4$ it amounts to 15%.

To make a practical use of the radial line, it is of interest to clarify the dependence of the transformation effect on the conditions of excitation of the line. The measurements have shown that the variation of the number of excitation points (n) weakly affects the pulse amplitude and shape for $n \gg 2(\pi R/c\eta)$. For example, for the

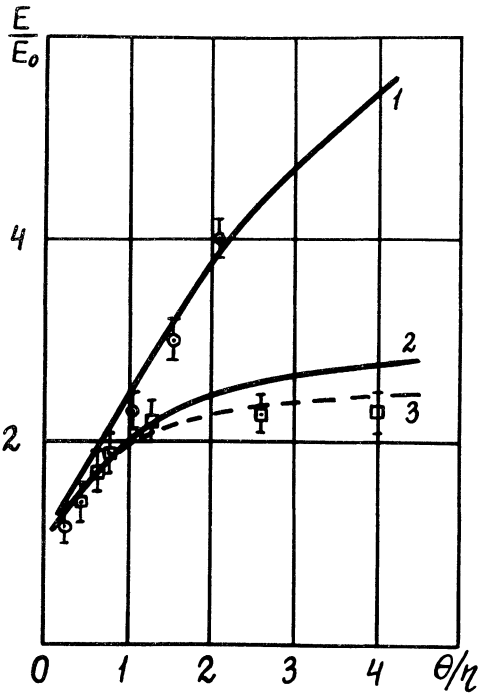

FIGURE 6 Electric field versus θ/η. (1) $r/R = 0$, $\tau_p/\theta = 0$; (2) $r/R = \frac{1}{3}$, $\tau_p/\theta = 0$; (3) $r/R = \frac{1}{3}$, $\tau_p/\theta = 0.067$. (⊙: without ferrite load; □: with ferrite load).

ferrite-loaded line with $R = 9$ cm at $\eta = 3$ ns, we obtain $2(\pi R/c\eta) \approx 0.6$, i.e., it is sufficient to use 2 or 3 excitation points.

To a greater extent, the transformation effect is influenced by the ratio of the source impedance ρ to the input resistance of the line, ρ_0. Two sets of the corresponding measurements were made for

i) the line without ferrite filler by varying ρ_0 from 1.3 to 9 ohms through changing the gap between its electrodes at a constant ρ of 2 ohms and also for

ii) the ferrite-loaded line varying ρ from 2 to 25 ohms with an appropriate choice of the number of feeder cables N at a constant ρ_0 of 40 ohms. The results of the latter measurements are given in Figure 7 (results of line measurements without ferrite are similar). It may be seen from the figure that the amplitude of the pulse decreases as N is reduced, and that it becomes flat-topped. This is explained by the change in the boundary conditions for electromagnetic wave travel and reflection at an external radial distance of the line. As a consequence of the continuously changing wave resistance of the line, as the wave propagates inward, there appear reflected waves propagating in the reverse direction. At low ρ/ρ_0, these waves, reaching the external radius R, form a reflected wave of the same amplitude but of opposite polarity. This wave, reaching the center of the line, leads to the electric field reduction, and this accounts for the pulse falloff with time (see Figure 7, $N = 24$). As the ρ/ρ_0 ratio grows,

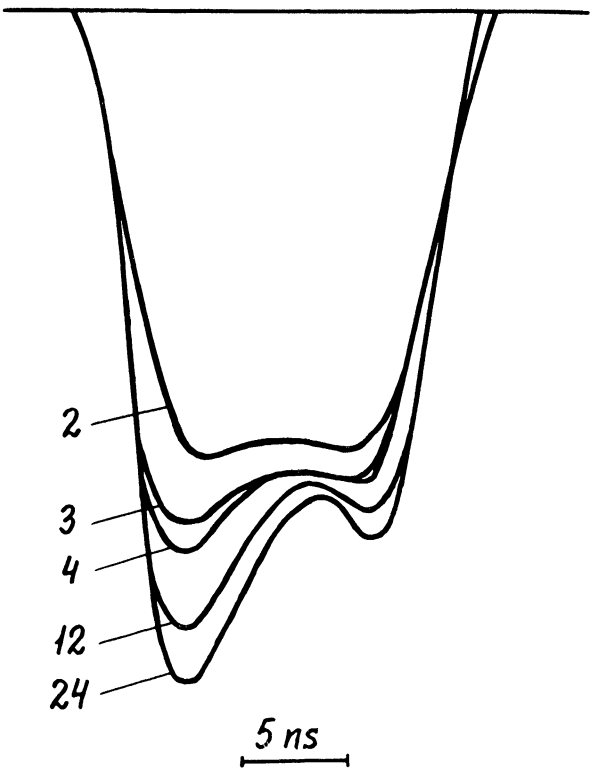

FIGURE 7 Oscilloscope traces of pulses in a ferrite-loaded radial line with a different number of feeder cables ($r/R = \frac{1}{3}$, $\eta \approx 2$ ns).

the amplitude of the reflected wave of opposite polarity diminishes, leading to a reduced pulse falloff with time ($N = 12, \ldots, 2$).

Thus, the results of the measurements show the possibility of obtaining flat-topped pulses in the center of the line via choosing the optimum ρ/ρ_0 ratio.

4 EXPERIMENTS IN HIGH-AMPLITUDE ELECTROMAGNETIC PULSE TRANSFORMATION AND INTERACTION WITH AN ELECTRON BEAM IN RADIAL LINES I

High-voltage pulse transformation experiments were performed using the device shown schematically in Figure 8. Here the voltage pulse of amplitude

$U = 20, \ldots, 40$ kV and risetime ranging from 1 to 10 ns comes from the pulse generator (3) via 50 ohm cables (2), 6 m long, to a system of radial lines (1). The 60 NN ferrite-loaded radial lines, 18 cm in outer diameter and 6 cm in inner diameter, were uniformly fed at 4 points on the circle. To sum pulses from several single radial lines, a system of double radial lines may be used, arranged either in line or

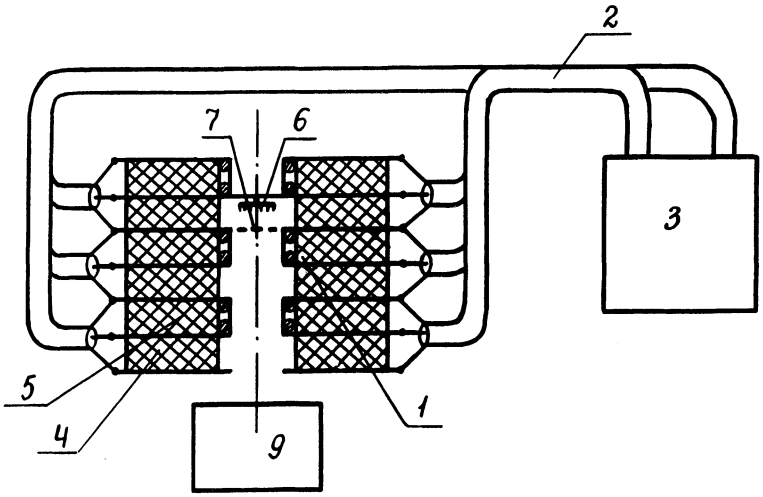

(a)

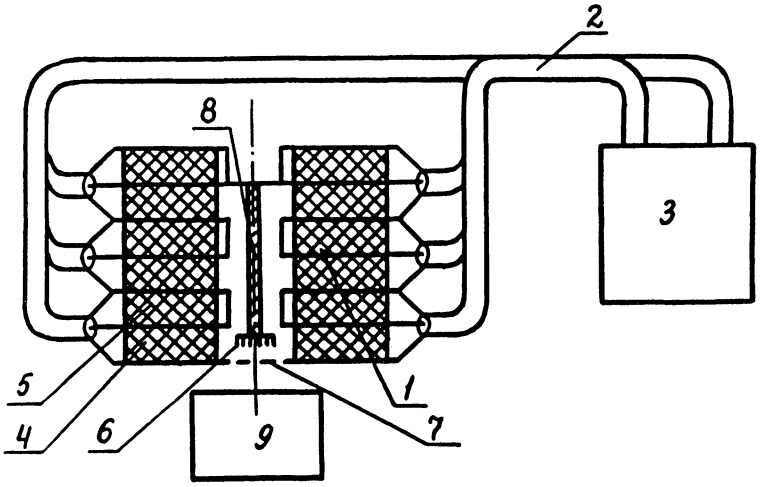

(b)

FIGURE 8 Experimental layout. (a) with beam transport, (b) without beam transport. (1) radial line system, (2) coaxial cables, (3) pulse voltage generator, (4) open-circuited radial line, (5) short-circuited radial line, (6) cathode, (7) anode-grid, (8) metal rod, (9) measuring system.

coaxially[1,8] and creating a non-potential electric field. In our experiments we used a sequence of open- (4) and short-circuited (near the axis) radial lines (5) forming double lines.

A burst-emission cathode (6) was used as a source of electrons. In our experiments it was placed either in the electric field of a single radial line (Figure 8a) or in the total electric field resulting from all the three radial lines (Figure 8b). In the first case, the beam, in passing along the axis of the three-line system, acquires an energy equal

to the sum of the accelerating voltages of each radial line. The beam is transported by a longitudinal pulsed magnetic field produced by coils (10) located in the short-circuited sections of the radial lines.[9] In the second case, the voltage pulses were summed by the use of a metal rod, at the end of which was mounted the cathode (6). By this means the cathode was placed in the total electric field of all the three radial lines.

The accelerated electron beam passing through the anode grid passed into the system (9) measuring beam current and energy. The beam current was measured by resistance pickups. Particle energy measurements were made using the aluminium-foil absorption technique and the electromagnetic analyzer. The latter was a plane capacitor with a homogeneous electric field inclined at an angle of 19.7° to the axis of the radial line array. A typical oscillograph trace of the beam curent pulse is shown in Figure 9.

In the experiments we studied the particle energy gain as functions of the beam current, and of the amplitude and rise time of the supply voltage pulse. Energy spectra of accelerated particles were also measured versus time.

The measured dependence of the particle energy on the pulse risetime at a pulse amplitude of 22 kV for the two cathode positions (see Figures 8a and b) is illustrated in Figure 10. (The same figure shows the electric field strengths calculated from these data for each accelerating gap). The measured data are in good agreement with the calculations (solid curve) at $\tau_\rho \approx 0$. Thus, at a large pulse amplitude the magnetic relaxation produces practically no effect on the transformation. As shown above (see Section 3), at a relatively low voltage $U = 1$ kV, magnetic relaxation in the ferrite leads to an appreciable decrease in the pulse amplitude on the line axis ($\tau_\rho = 0.3$ ns). These results can be explained by the known fact that magnetic relaxation time

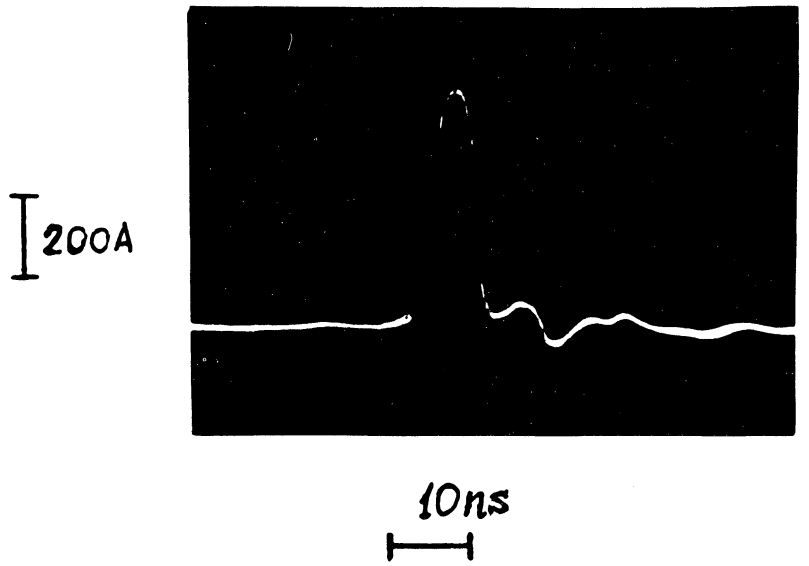

FIGURE 9 Oscilloscope trace of the beam current pulse.

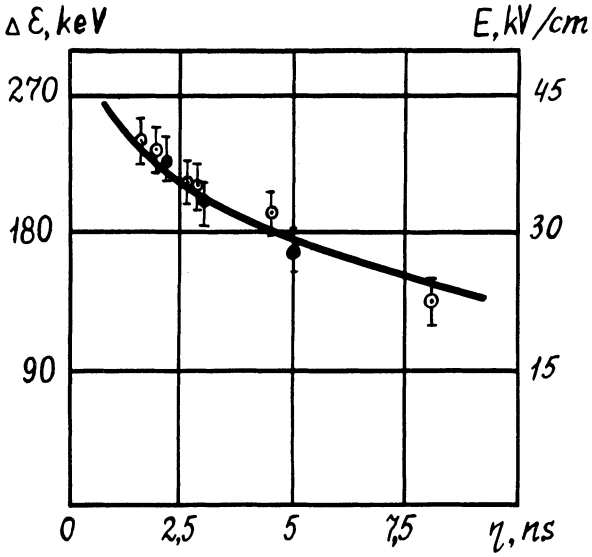

FIGURE 10 Gain in the particle energy and electric field strength in the gap as a function of the pulse rise time at the line input ($U = 22$ kV). ⊙: layout of Figure 8a; ●: layout of Figure 8b.

decreases with the magnetizing magnetic field (e.g., see Ref. 10). In our case, the magnetic field was that of the pulse.

The present measurements have demonstrated the dependence of the particle energy gain on the amplitude of the supply voltage pulse to be linear up to U 40 kV, in agreement with the calculation. At $U = 38$ kV and $\eta \approx 1.5$ ns, the three-line system gave a particle energy gain of 360 keV. This corresponds to an electric field strength in the gaps of 60 kV/cm.

The results obtained are in agreement with the single-line measurements, i.e., the particle energy gain in three radial lines is equal to a three-fold energy gain in a single radial line.

The energy vs. time measurements of the electron beam produced and accelerated in the three-line system were carried out with the electrostatic analyzer. Time dependences of the beam current during the pulse were measured, the beam particle energies being greater than an assigned ε_b value. It was found that, with increasing ε_b, the pulse time is reduced and is 2 or 3 ns at large ε_b values. This is in agreement with the results of the theoretical analysis.

The inverse effect of the beam on the transformation processes was studied by measuring the maximum particle energy gain as a function of the beam current. Based on these measurements, we have plotted the particle energy gain as a generalized function of the beam resistance $R_b = \varepsilon/eI$, resulting in the curve shown in Figure 11. From this plot one can determine the beam current below which the particle energy gain does not vary significantly. For example, at $U = 38$ kV, reduction in the particle energy at 10% takes place at a beam current of about 400 A. Hence, in radial lines loaded with type 60 NN ferrite, beams with currents of hundreds of amperes can be accelerated efficiently.

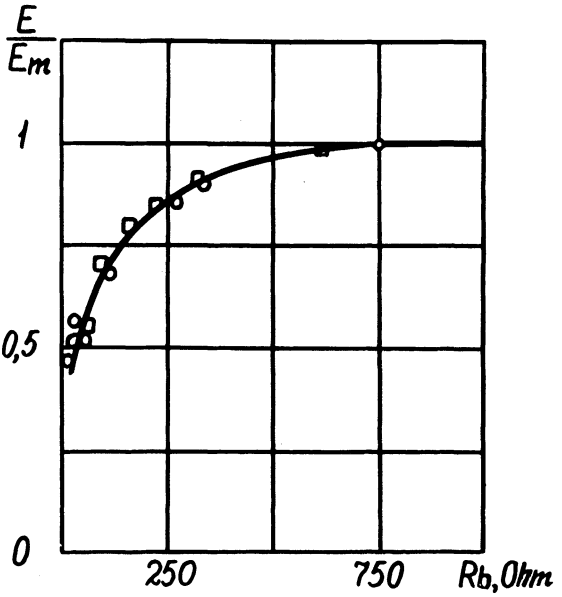

FIGURE 11 Generalized dependence of the electric field amplitude on the beam resistance $R_b = \varepsilon/eI$. ○: beam measurements; □: measurements with the resistance simulating the beam.

5 TIME TRANSFORMATION OF PULSES IN A RADIAL LINE

The analysis undertaken in Section 2 has shown that, in propagating from the periphery to the center of the radial line, the pulse changes not only in its amplitude but also in its shape. For example, at $\theta/\eta = 4.5$ and $T/\theta = 0.22$, the pulse length at the base diminishes by 30%, while the falloff time decreases by a factor of 3 (see Figure 2). We discuss this problem in more detail below.

For this purpose, we define the electric-field pulse shape at the input of the line that is necessary to obtain, for the accelerating field, a trapezoidal pulse of amplitude E_{co}, flat-time 2Λ, and rise and fall time τ on the line axis. Substituting into Eq. (5) the Fourier-transformed image of this pulse,

$$E_{\omega c} = \frac{E_{co}}{2\pi\tau\omega^2}\{e^{-i\omega\tau} + e^{-i\omega(\tau+\Lambda)} - e^{-i\omega(2\tau+\Lambda)} - 1\}, \tag{11}$$

by simple manipulations we get

$$\frac{t}{\theta} \leq -1 - \frac{\Lambda}{\theta} - \frac{\tau}{\theta} \quad E_{1i} = 0$$

$$-1 - \frac{\Lambda}{\theta} - \frac{\tau}{\theta} \leq \frac{t}{\theta} \leq -1 - \frac{\Lambda}{\theta} \; E_{1i} = E_{co}\frac{\theta}{\pi\tau}\left\{\frac{t+\Lambda+\tau}{\theta}\left[\frac{\pi}{2}\right.\right.$$

$$\left.\left. + \arcsin\frac{t+\Lambda+\tau}{\theta}\right] + \sqrt{1-\left(\frac{t+\Lambda+\tau}{\theta}\right)^2}\right\};$$

$$-1-\frac{\Lambda}{\theta}\le\frac{t}{\theta}\le-1+\frac{\Lambda}{\theta}\quad E_{1i}=E_{co}\frac{\theta}{\pi\tau}\left\{\frac{\pi\tau}{2\theta}+\frac{t+\Lambda+\tau}{\theta}\arcsin\frac{t+\Lambda+\tau}{\theta}\right.$$
$$\left.+\sqrt{1-\left(\frac{t+\Lambda+\tau}{\theta}\right)^2}-\sqrt{1-\left(\frac{t+\Lambda}{\theta}\right)^2}-\frac{t+\Lambda}{\theta}\arcsin\frac{t+\Lambda}{\theta}\right\};$$

$$-1+\frac{\Lambda}{\theta}\le\frac{t}{\theta}\le1+\frac{\Lambda}{\theta}+\frac{\tau}{\theta}\quad E_{1i}=E_{co}\frac{\theta}{\pi\tau}\left\{\frac{t+\Lambda+\tau}{\theta}\arcsin\frac{t+\Lambda+\tau}{\theta}\right.$$
$$+\sqrt{1-\left(\frac{t+\Lambda+\tau}{\theta}\right)^2}-\frac{t+\Lambda}{\theta}\arcsin\frac{t+\Lambda}{\theta}-\sqrt{1-\left(\frac{t-\Lambda}{\theta}\right)^2}$$
$$\left.-\frac{\pi}{2}\left(\frac{t-\Lambda-\tau}{\theta}\right)-\frac{t-\Lambda}{\theta}\arcsin\frac{t-\Lambda}{\theta}\right\};$$

$$-1+\frac{\Lambda}{\theta}+\frac{\tau}{\theta}\le\frac{t}{\theta}\le1-\frac{\Lambda}{\theta}-\frac{\tau}{\theta}\quad E_{1i}=E_{co}\frac{\theta}{\pi\tau}\left\{\frac{t+\Lambda+\tau}{\theta}\arcsin\frac{t+\Lambda+\tau}{\theta}\right.$$
$$+\sqrt{1-\left(\frac{t+\Lambda+\tau}{\theta}\right)^2}-\sqrt{1-\left(\frac{t+\Lambda}{\theta}\right)^2}-\frac{t+\Lambda}{\theta}\arcsin\frac{t+\Lambda}{\theta}$$
$$+\sqrt{1-\left(\frac{t-\Lambda-\tau}{\theta}\right)^2}-\sqrt{1-\left(\frac{t-\Lambda}{\theta}\right)^2}+\frac{t-\Lambda-\tau}{\theta}\arcsin\frac{t-\Lambda-\tau}{\theta}$$
$$\left.-\frac{t-\Lambda}{\theta}\arcsin\frac{t-\Lambda}{\theta}\right\};$$

$$1-\frac{\Lambda}{\theta}-\frac{\tau}{\theta}\le\frac{t}{\theta}\le1-\frac{\Lambda}{\theta}\quad E_{1i}=E_{co}\frac{\theta}{\pi\tau}\left\{\frac{\pi}{2}\left(\frac{t+\Lambda+\tau}{\theta}\right)-\frac{t+\Lambda}{\theta}\arcsin\frac{t+\Lambda}{\theta}\right.$$
$$-\sqrt{1-\left(\frac{t+\Lambda}{\theta}\right)^2}+\frac{t-\Lambda-\tau}{\theta}\arcsin\frac{t-\Lambda-\tau}{\theta}+\sqrt{1-\left(\frac{t-\Lambda-\tau}{\theta}\right)^2}$$
$$\left.-\sqrt{1-\left(\frac{t-\Lambda}{\theta}\right)^2}-\frac{t-\Lambda}{\theta}\arcsin\frac{t-\Lambda}{\theta}\right\};\qquad(12)$$

$$1-\frac{\Lambda}{\theta}\le\frac{t}{\theta}\le1+\frac{\Lambda}{\theta}\quad E_{1i}=E_{co}\frac{\theta}{\pi\tau}\left\{\frac{\pi}{2}\frac{\tau}{\theta}+\frac{t-\Lambda-\tau}{\theta}\arcsin\frac{t-\Lambda-\tau}{\theta}\right.$$
$$\left.+\sqrt{1-\left(\frac{t-\Lambda-\tau}{\theta}\right)^2}-\sqrt{1-\left(\frac{t-\Lambda}{\theta}\right)^2}-\frac{t-\Lambda}{\theta}\arcsin\frac{t-\Lambda}{\theta}\right\};$$

$$1+\frac{\Lambda}{\theta}\le\frac{t}{\theta}\le1+\frac{\Lambda}{\theta}+\frac{\tau}{\theta}\quad E_{1i}=E_{co}\frac{\theta}{\pi\tau}\left\{\frac{t-\Lambda-\tau}{\theta}\arcsin\frac{t-\Lambda-\tau}{\theta}-\frac{\pi}{2}\left(\frac{t-\Lambda-\tau}{\theta}\right)\right.$$
$$\left.+\sqrt{1-\left(\frac{t-\Lambda-\tau}{\theta}\right)^2}\right\};$$

$$1+\frac{\Lambda}{\theta}+\frac{\tau}{\theta}\le\frac{t}{\theta}\quad E_{1i}=0.$$

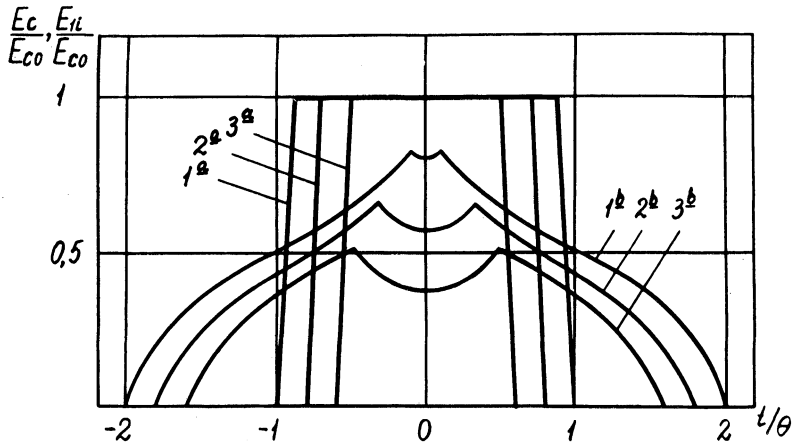

FIGURE 12 Time dependence of the electric field on the axis (1a, 2a, 3a) and at the input of the radial line (1b, 2b, 3b) for $\tau/\theta = 0.1$ and $\Lambda/\theta = 0.9$ (1), 0.7 (2), and 0.5 (3).

Some results of the calculations by Eqs. (12) are given in Figure 12. It is seen from the figure that to have electric field pulses with short rise time and a flat top (of type 1a to 3a) on the axis of the radial line, pulses of a particular shape (see 1b to 3b) must be supplied to the line input. In this case, we observe an essential reduction in the length of the pulse and its edges. For example, at $2\Lambda = \theta$, $\tau = 0.1\theta$, the pulse time diminishes by a factor of 3.5, and the rise time by a factor of 11.

The calculations predict the possibility of even a greater reduction of the pulse time. Thus, for $2\Lambda = 0.05\theta$ and $\tau = 0.05\theta$, the pulse time may be reduced by a factor of 7.5, e.g., from 3 ns down to 0.4 ns. Note also that a substantial change of the voltage pulse shape at the line input (from 1b to 3b in Figure 11) causes only a small change in the flat-top time of the pulse on the line axis (curves 1a to 3a). From Eqs. (12) it follows that the transformation of the pulse and edge times is determined by the ratio of these paramters to the transit time of the wave along the line.

For the case of long pulses, after integration in Eq. (10), we obtain

$$\frac{t}{\theta} \leq -1\frac{\Lambda}{\theta} - \frac{\tau}{\theta} \quad E_{1i} = 0$$

$$-1 - \frac{\Lambda}{\theta} - \frac{\tau}{\theta} \leq \frac{t}{\theta} \leq -1 - \frac{\Lambda}{\theta} \quad E_{1i} = E_{co}\frac{\theta}{\pi\tau}\left\{\frac{t+\Lambda+\tau}{\theta}\left[\frac{\pi}{2} + \arcsin\frac{t+\Lambda+\tau}{\theta}\right]\right.$$

$$\left. + \sqrt{1 - \left(\frac{t+\Lambda+\tau}{\theta}\right)^2}\right\};$$

$$-1 - \frac{\Lambda}{\theta} \leq \frac{t}{\theta} \leq 1 - \frac{\Lambda}{\theta} - \frac{\tau}{\theta} \quad E_{1i} = E_{co}\frac{\theta}{\pi\tau}\left\{\frac{\pi}{2}\frac{\tau}{\theta} + \frac{t+\Lambda+\tau}{\theta}\arcsin\frac{t+\Lambda+\tau}{\theta}\right.$$

$$\left. - \sqrt{1 - \left(\frac{t+\Lambda}{\theta}\right)^2} - \left(\frac{t+\Lambda}{\theta}\right)\arcsin\frac{t+\Lambda}{\theta} + \sqrt{1 - \left(\frac{t+\Lambda+\tau}{\theta}\right)^2}\right\};$$

$$1-\frac{\Lambda}{\theta}-\frac{\tau}{\theta}\le\frac{t}{\theta}\le 1-\frac{\Lambda}{\theta}\quad E_{1i}=E_{co}\frac{\theta}{\pi\tau}\left\{\frac{\pi}{2}\left(\frac{t+\Lambda+2\tau}{\theta}\right)-\left(\frac{t+\Lambda}{\theta}\right)\arcsin\frac{t+\Lambda}{\theta}\right.$$

$$\left.-\sqrt{1-\left(\frac{t+\Lambda}{\theta}\right)^2}\right\};\qquad(13)$$

$$1-\frac{\Lambda}{\theta}\le\frac{t}{\theta}\le -1+\frac{\Lambda}{\theta}\quad E_{1i}=E_{co};$$

$$-1+\frac{\Lambda}{\theta}\le\frac{t}{\theta}\le -1+\frac{\Lambda}{\theta}+\frac{\tau}{\theta}\quad E_{1i}=E_{co}\frac{\theta}{\pi\tau}\left\{-\frac{\pi}{2}\left(\frac{t-\Lambda-2\tau}{\theta}\right)-\frac{t-\Lambda}{\theta}\arcsin\frac{t-\Lambda}{\theta}\right.$$

$$\left.-\sqrt{1-\left(\frac{t-\Lambda}{\theta}\right)^2}\right\}$$

$$-1+\frac{\Lambda}{\theta}+\frac{\tau}{\theta}\le\frac{t}{\theta}\le 1+\frac{\Lambda}{\theta}\quad E_{1i}=E_{co}\frac{\theta}{\pi\tau}\left\{\frac{\pi}{2}\frac{\tau}{\theta}+\frac{t-\Lambda-\tau}{\theta}\arcsin\frac{t-\Lambda-\tau}{\theta}\right.$$

$$\left.+\sqrt{1-\left(\frac{t-\Lambda-\tau}{\theta}\right)^2}-\sqrt{1\quad\left(\frac{t-\Lambda}{\theta}\right)^2}-\frac{t-\Lambda}{\theta}\arcsin\frac{t-\Lambda}{\theta}\right\}$$

$$1+\frac{\Lambda}{\theta}\le\frac{t}{\theta}\le 1+\frac{\Lambda}{\theta}+\frac{\tau}{\theta}\quad E_{1i}=E_{co}\frac{\theta}{\pi\tau}\left\{-\frac{\pi}{2}\left(\frac{t-\Lambda-\tau}{\theta}\right)\right.$$

$$\left.+\frac{t-\Lambda-\tau}{\theta}\arcsin\frac{t-\Lambda-i}{\theta}+\sqrt{1-\left(\frac{t-\Lambda-\tau}{\theta}\right)^2}\right\};$$

$$1+\frac{\Lambda}{\theta}+\frac{\tau}{\theta}\le\frac{t}{\theta}\quad E_{1i}=0.$$

Some results of the calculations by Eqs. (13) are depicted in Figure 13. It is seen that the time of the long pulse actually undergoes no transformation, though

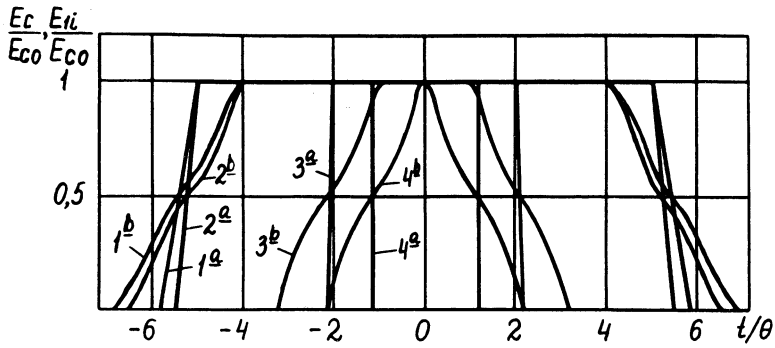

FIGURE 13 Time dependence of the electric field on the axis (a) and at the input (b) of the radial line. (1) $\Lambda/\theta = 5$, $\tau/\theta = 0.8$; (2) $\Lambda/\theta = 5$, $\tau/\theta = 0.5$; (3) $\Lambda/\theta = 2$, $\tau/\theta = 0.1$; (4) $\Lambda/\theta = 1.1$, $\tau/\theta = 0.1$.

there is an essential reduction in the risetime. For example, at $\tau = 0.1\theta$, the pulse propagates from the periphery inward, and its risetime is reduced by a factor of 15. According to our analysis, this time-transformation effect depends only on the ratio of the risetime to the wave-transit time.

The results presented above were obtained for the source impedance $\rho = 0$ and were found to be practically the same at $\rho \leq 30$ d/R (ohm).

It is evident from the analysis that sub-nanosecond pulses of the accelerating field with short risetimes can be generated on the axis of the radial line by driving this line with relatively long pulses that have comparatively long risetimes.

Some basic regularities of the time transformation of pulses in the radial line—in particular, possible attainment of short-time accelerating fields, were confirmed experimentally. The measurements were made on a device similar to that of Section 3. The data obtained for the case of time pulses are represented in Figure 14. It is seen from the figure that the input pulse has nearly a triangular shape, with rise and fall time of ≈ 5.5 ns, and that pulse on the line axis has practically a trapezoidal shape with $\tau \approx 2$ ns and the flat-top time ≈ 4 ns. There is good agreement between calculations and measurements. Some discrepancies observed may be attributed to the input pulse shape being somewhat different from that calculated by Eqs. (12). This discrepancy is insignificant, and therefore, when the line is driven with pulses having exponential rise and fall, which is easily realizable in practice, there occurs an important transformation of both the pulse time and the rise and fall times.

Figure 15 shows the measured transformation of the pulse rise time τ. As is seen, the experimental data are in agreement with the calculation and confirm the

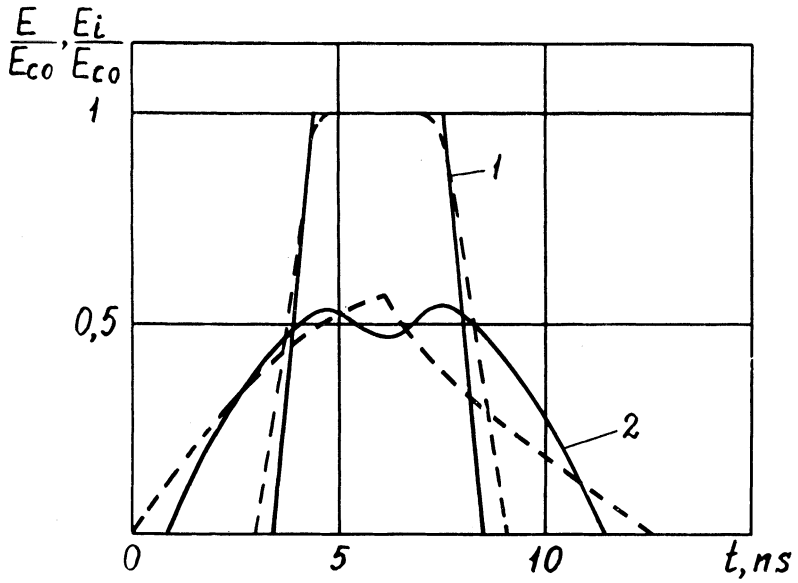

FIGURE 14 Measured (dashed line) and calculated (solid line) data for the case of short pulses. (1) pulses on the axis, (2) input pulses.

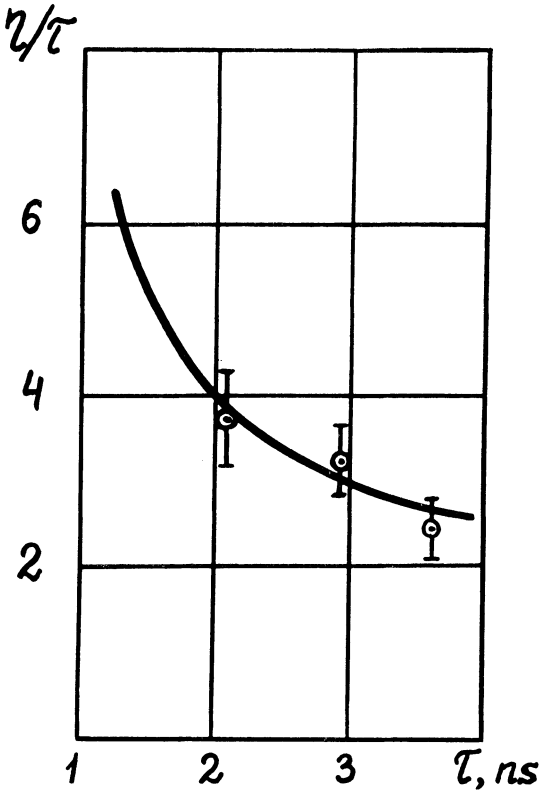

FIGURE 15 Transformation of the electric field on the line axis as a function of its rise time at the input of the radial line (for $\tau < \theta < \Lambda$). Solid line represents the calculations, dots show measurements.

conclusion about possible significant reduction of τ. For example, the pulse rise time of about 8 ns at the line input is reduced to ≈ 2 ns as the pulse propagates to the axis of the line.

6 CONCLUSIONS

We have studied the physical processes occurring during propagation of short electromagnetic pulses in radial transmission lines. Pulse amplitude-transformation and time-transformation effects are demonstrated to take place in the radial line. It is found that the amplitude transformation value depends on the ratio of the wave-transit time to the electric field build-up time at the line input. In the case of a ferrite-loaded radial line, this transformation also depends on the ratio of the magnetic relaxation time of the ferrite to the wave-transit times. It is demonstrated that electron beams of currents of hundreds of amperes can efficiently be accelerated in radial lines with ferrite loading. A system of three double radial lines of a total length of 12 cm gave a 360-keV particle energy gain at a supply voltage of 38 kV.

It is also shown that, with the propagation of short pulses in the radial line, the pulse duration and rise and fall times are reduced. This can be used to obtain short (sub-nanosecond) accelerating pulses. In the case of long pulses, only rise and fall times are reduced. The time transformation effect is determined only by the ratio of the pulse time and rise time to the wave-transit time.

REFERENCES

1. E. C. Hartwig, *Symposium of Electron Ring Accelerators*, Lawrence Berkeley Laboratory Report UCRL-18108 TID-4500 (1968) pp. 44–64.
2. V. I. Kazacha and I. V. Kozhukhov, *Zh. Tekh. Fiz.* **46**, 1477 (1976).
3. V. V. Zakutin and A. M. Shenderovich, "On accelerating high-current electron beams by the use of radial lines" (in Russian) collected in Voprosy Atomnoj Nauki i Tekhniki, ser. Linejnye uskoriteli (Kharkov, KhFTI) **2**, 5 (1977) 53.
4. J. Smith, *Rev. Sci. Instrum.* **50**, 714 (1979).
5. M. E. Jones, *Part. Accel.* **21**, 43 (1987).
6. Petr *et al.*, *Rev. Sci Instrum.* **59**, 132 (1988).
7. A. G. Gurevich, Ferrites at superhigh frequencies (in Russian) (GIFML, Moscow, 1960), p. 407.
8. V. V. Zakutin, B. G. Safronov and A. M. Shenderovich, "An accelerating system" (in Russian), Inventor's Certificate N713 511 (USSR), published in *Byull. Izobret.* **N29** (1981).
9. V. V. Zakutin and A. M. Shenderovich, "A device for generating a pulsed magnetic field" (in Russian), Inventor's Certificate N 517 192 (USSR), published in *Byull. Izobret.* **N21** (1976).
10. J. Smith and H. P. J. Wijn, *Ferrites* (Russian translation) (Inostr. Lit., Moscow, 1962).
11. *Ferrites Handbook* (in Russian) (Sow Radio, Moscow, 1968).